



Contents lists available at ScienceDirect

Journal of Biomechanics

journal homepage: www.elsevier.com/locate/jbiomech
www.JBiomech.com

Experiments on dynamic behaviour of a Dacron aortic graft in a mock circulatory loop

Giovanni Ferrari^a, Prabhakaran Balasubramanian^a, Eleonora Tubaldi^b, Francesco Giovanniello^a, Marco Amabili^{a,*}^a Dept. of Mechanical Engineering, McGill University, Macdonald Engineering Building, 817 Sherbrooke St. W, Montreal H3A 0C3, Quebec, Canada^b Department of Aerospace and Mechanical Engineering, University of Arizona, 1130 N. Mountain Ave., Tucson AZ 85721, USA

ARTICLE INFO

Article history:

Accepted 30 January 2019

Keywords:

Dacron graft
Aortic graft
Mock circulatory loop
Dynamic behaviour
Experiment

ABSTRACT

Woven Dacron grafts are currently used for the surgical treatment of aortic aneurysm and acute dissection, two otherwise fatal pathologies when aortic wall rupture occurs. While Dacron is chosen for aortic grafts because of characteristics such as biocompatibility and durability, few data are available about the dynamic response of Dacron prosthetic devices and about their side effects on the cardiovascular system. In this study, a Dacron graft was subjected to physiological flow conditions in a specifically-developed mock circulatory loop. Experiments were conducted at different physiological pulsation-per-minute rates. Results show that, in comparison to an aortic segment of the same length, the prosthesis is extremely stiffer circumferentially, thus limiting the dynamical radial expansion responsible for the Windkessel effect in human arteries. The prosthesis is instead excessively compliant in the axial direction and develops preferentially bending oscillations. This very different dynamic behaviour with respect to the human aorta can alter cardiovascular pressure and flow dynamics resulting in long-term implant complications.

© 2019 Elsevier Ltd. All rights reserved.

1. Introduction

Dacron is the commercial name for polyethylene terephthalate, also known as polyester. A bibliography regarding the use of Dacron prostheses in the context of aortic surgery can be found in (Thompson, 1998). Collagen impregnation was introduced to reduce postoperative internal bleeding and to favor endothelial seeding (Dalsing et al., 1989). Dacron grafts are linked to a satisfyingly low rate of complications, mostly consisting in graft dilatation and mechanical failure. However, an increasing number of researchers (Spadaccio et al., 2013) supposes that the many-times larger circumferential stiffness of grafts with respect to the human aorta (Tremblay et al., 2009) may perturbate the Windkessel effect, the arterial dynamics and consequently the ventricular load. The discontinuity at the sutures at the interface between the graft and the remaining aortic portion may cause pressure wave reflections that can dramatically increase heart workload.

Woven Dacron is a composite material where a fabric constituted by continuous strands of polymeric fibres is immersed in a protein matrix (collagen). Woven Dacron also presents direction

and time-dependent mechanical behavior. The static mechanical properties of Dacron were investigated by several researchers (Bustos et al., 2016a; Hasegawa and Azuma, 1979; How, 1992; Yeoman et al., 2010). The relaxation of this material at low strain rates was also investigated (Lee and Wilson, 1986). Amabili et al. (2018) experimentally investigated the static, relaxation and dynamic mechanical behaviour of woven Dacron for commercial aortic grafts. They found a large increase of the dynamic stiffness with respect to the static stiffness, which is very relevant since prostheses are subjected to dynamic loading (i.e. physiological pulsatile flow and pressure). The effect of static pressurization on Dacron graft was studied by Bustos et al. (2016b). A finite-element fluid-structure interaction for Dacron grafts was developed by Jayendiran et al. (2018). The nonlinear dynamic response of a Dacron graft to pulsatile flow was analytically and numerically investigated by Tubaldi et al. (2018).

Mock circulatory loops (MCLs) are an essential asset for the *in vitro* testing of cardiovascular devices subjected to pulsatile blood flow. Pulsatile piston pumps became soon a widespread option used to recreate the physiological ventricular pumping characteristics in this type of apparatus. Several studies show attempts to recreate desired pulsatile flow conditions through the usage of electromechanical systems under closed loop control.

* Corresponding author.

E-mail address: marco.amabili@mcgill.ca (M. Amabili).

Taylor and Miller produced a series of papers about the closed-loop automatic control of the entire MCLs and the three main components of MCLs: the pulsatile pump, the expansion chamber with an air cushion to reproduce the Windkessel effect and pinch valves to recreate the peripheral resistance (Taylor et al., 2012; Taylor and Miller, 2012a, 2012b). Their choice was an Harvard Apparatus piston pump, which is still considered a high-end solution.

To the authors' knowledge, MCLs have never been used to test the effects of Dacron implants on the human circulatory system. In this study, the behavior of the woven Dacron prosthesis is tested in a mock circulatory loop for the first time. The understanding of the dynamics of cardiovascular prostheses is crucial to identify the limitations of the currently used prostheses in mimicking the dynamic expansion of the lumen of the human aorta. This study highlights that the insertion of a woven Dacron prosthesis in the arterial tree reduces extremely the Windkessel effect and bending vibrations are generated. As a result, this compromises the functioning of the vasculature and leads to an increase in the heart workload (Spadaccio et al., 2013).

2. Materials and methods

2.1. Woven Dacron graft

A thin woven Dacron fabric has different properties in two perpendicular in-plane directions and can be considered as an orthotropic material. In the axial direction a corrugation is present in woven Dacron grafts to increase the axial compliance and to facilitate non-straight implantation. A Hemashield Platinum woven double velour thoracic aortic prosthesis produced by Maquet was experimentally studied; this is a collagen-impregnated graft.

According to the producer, the nominal length is 300 mm and the nominal diameter is 28 mm. The geometrical details and dimensions are shown in Fig. 1.

The prosthesis was cut by means of straight surgical scissors between two ridges at a length of 110 ± 1 mm in the unloaded state. The middle-surface diameter was measured to be 27.8 ± 0.4 mm by cutting a thin cylindrical ring from the prosthesis, opening it and measuring its length. The cut portion presents 62 corrugation waves along the axis. The axial length of one wave is 1.77 ± 0.05 mm. The thickness of the fabric is 0.33 ± 0.01 mm and was measured with a Vernier caliper. When implanted, the prosthesis is subjected to an axial prestress and internal pressure. Indeed, the human aorta retracts to a shorter length if excised and the axial pre-stretch depends on age (Horný et al., 2014). An axial stretch of 1.3 times the undeformed length of the graft was chosen during tests in the mock circulatory loop.

2.2. Static and dynamic mechanical properties of woven Dacron

Amabili et al. (2018) characterized the static and viscoelastic behavior of woven Dacron strips taken from Hemashield Platinum aortic grafts. In Amabili et al. (2018), the axial strip was characterized after pre-stretch to remove the corrugation. Since the studied graft presents corrugations, the static strain-stress curves in axial and circumferential directions were tested again without any axial pre-stretch in both cases, and results are reported in Fig. 2(a and b). The 2nd Piola-Kirchhoff stresses σ and Green's strains ε are obtained as

$$\sigma = \frac{F}{A\lambda}, \quad \varepsilon = \frac{\Delta L}{L} + \frac{1}{2} \left(\frac{\Delta L}{L} \right)^2, \quad (1a, b)$$

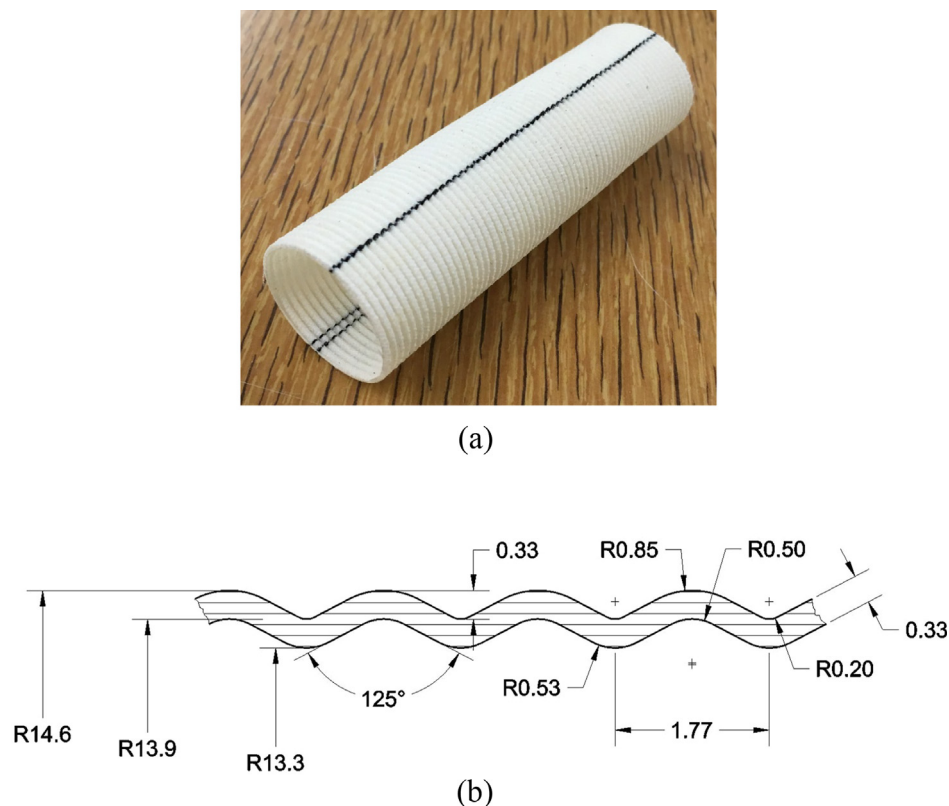


Fig. 1. (a) Dacron graft under test; (b) characteristic dimensions of the wave structure of the tested Dacron graft.

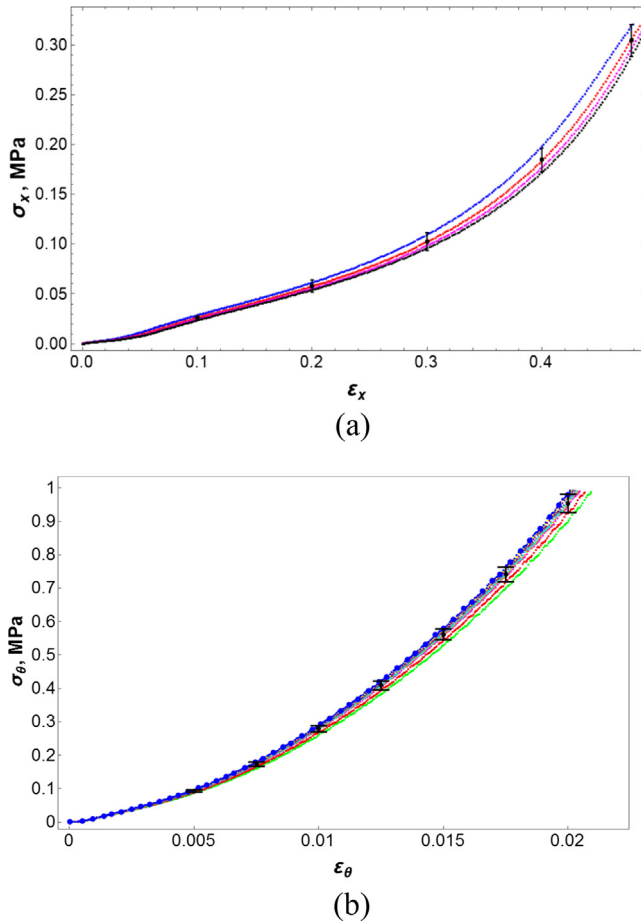


Fig. 2. Uniaxial tensile tests on strips from a woven Dacron aortic graft; 2nd Piola-Kirchhoff stress, Green strain. (a) Axial strip, four repeated tests, mean values and standard deviations; (b) circumferential strip, nine repeated tests, mean values and standard deviations (Amabili et al., 2018).

where F is the measured force, A is the cross-section area, $\lambda = 1 + \Delta L/L$ is the stretch, ΔL is the elongation caused by the applied force F and L is the original length of the strip. Here it must be clarified that, since the cross-section area is non-continuous with fibers having space among them, a conventional continuous cross-section without pores is assumed. Therefore, the stress given by Eq. (1a) is a conventional value. A second reason for the difference between Eq. (1a) and the actual stress value in the fibers is due to the geometry of the Dacron graft along the longitudinal axis, which is shown in Fig. 1(b). This introduces stress concentrations.

Fig. 2(a and b) were obtained by using an *eXpert 4000 Admet Micro Test System* after ten pre-conditioning cycles on strips of 45×10.5 mm at a strain rate of 0.025 mm/s. Fig. 2(b) coincides with the one obtained in Amabili et al. (2018). Results indicate a very high circumferential and a very low axial stiffness of the corrugated Dacron.

The experimental frequency-dependent stiffness and dissipation characteristics of a viscoelastic material can be described by the *complex modulus*. Under harmonic oscillations, the ratio between stress and strain for a viscoelastic material is a frequency dependent complex number. This is justified by the fact that, depending on the forcing frequency, a phase ϕ is present between the imposed dynamic force and the resulting elongation. Through the measurement of (i) the dynamic force, (ii) the corresponding elongation of a Dacron strip and (iii) the phase between the two, the amplitude of the complex modulus can be obtained as

$$|E^*| = \frac{|\Delta f|/A}{|\Delta l|/L} \frac{1}{\lambda^2}, \quad (2)$$

where, L is the original free length of the strip and A its cross-section area, both before applying the pre-stretch λ . The reason for the presence of the term $1/\lambda^2$ in Eq. (2) is to convert the complex modulus from the slope of the engineering stress/engineering strain curve to the slope of the 2nd Piola-Kirchhoff stress/Green's strain curve. The storage modulus E' and the loss modulus E'' are given by

$$E' = |E^*| \cos \phi, \quad E'' = |E^*| \sin \phi, \quad (3a, b)$$

the loss factor η is

$$\eta = \tan \phi. \quad (4)$$

The experiments were carried out at assigned initial pre-stretches on one axial and one circumferential Dacron strip. The values of pre-stretch and the corresponding stresses are presented in Table 1. The stretches were chosen in order to reach physiological stresses. A strip holder was connected to a fix surface through a *Brüel & Kjær 8203* piezoelectric load cell. The other strip holder was fixed to the armature of a *Brüel & Kjær 4824* electrodynamic exciter connected to a *Brüel & Kjær 2732* power amplifier and controlled by a LMS/Siemens Test-Lab system; its dynamic displacement was measured by a Polytec OFV-505 laser Doppler vibrometer with displacement decoder. The harmonic excitation was varied from 1 to 60 Hz with an adaptive frequency resolution varying from 0.1 to 0.5 Hz. The initial 50 cycles at every frequency were discarded to eliminate the transient vibration and give pre-conditioning. The dynamic elongation Δl and the dynamic harmonic force Δf applied to the strip, of the order of 0.1 N, were measured for 10 cycles. A small dynamic load, superimposed to the static load, allows for a linear response of the material around the pre-stretched configuration. This linear relationship is used in Eq. (2) to find the complex modulus. The estimation of measurement errors is presented in Appendix A.

2.3. Mock circulatory loop

A mock circulatory loop was designed and built for this application and its scheme is shown in Fig. 3(a). A photo of the test section with the Dacron graft installed and equipped with Carolina Medical magnetic flowmeters and Millar catheter pressure sensors at the inlet and outlet of the prosthesis is shown in Fig. 3(b). A classical, manually controlled design was developed to recreate the pumping action of the heart and the Windkessel effect for the portion of the arterial tree. The pumping action of the heart is recreated by a model 55-3305 piston pump by Harvard Apparatus. The pump is in a standard configuration, with ball check valves and manual controls of stroke (range 15–100 cc), systole/diastole ratio (25/75 to 50/50 %) and analogic speed control. The maximum speed of this pump is limited to 100 beats per minute (bpm). However, in this case the standard Bodine 6126 electric motor was substituted by a Bodine 6125 motor capable of an approximately double speed. This allows to study the full range of physiological heart rates.

3/4" ID tygon tubing was employed. The Dacron prosthesis is assumed to replace a long portion of the thoracic descending aorta

Table 1

Pre-stretch values and associated stresses applied in the dynamic characterization of axial and circumferential strips from a woven Dacron aortic graft.

Axial strip		Circumferential strip	
Stretch	Stress (MPa)	Stretch	Stress (MPa)
1.22	0.08	1.008	0.17
1.29	0.16	1.01	0.25
1.36	0.30	1.012	0.40

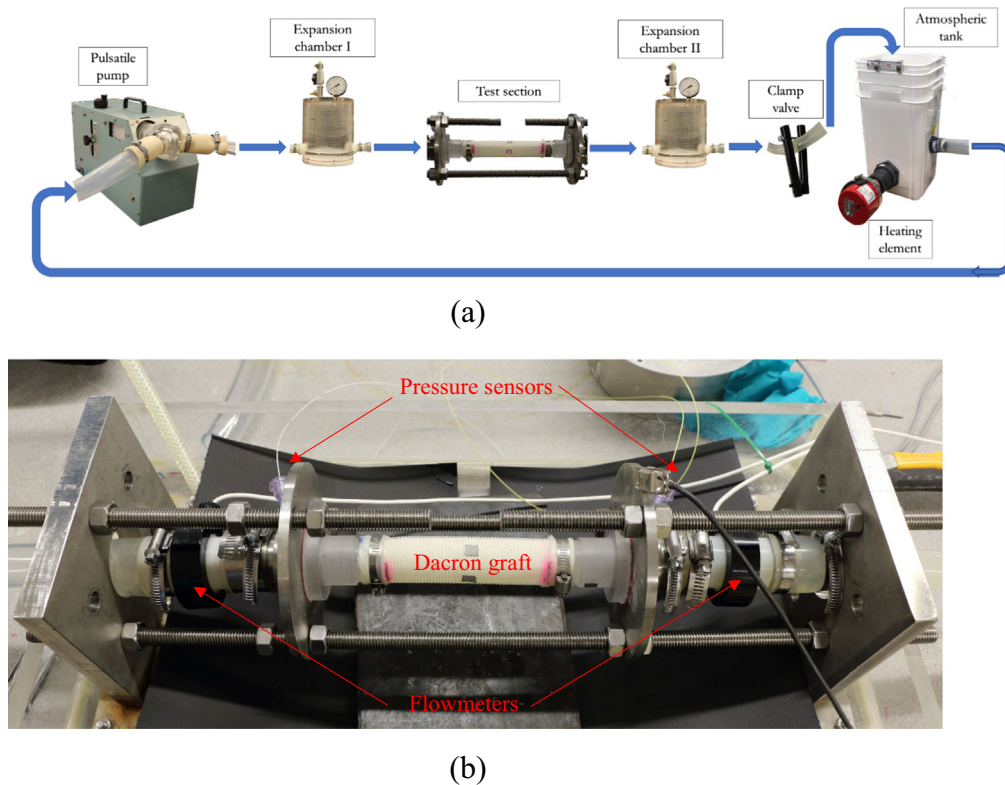


Fig. 3. Mock circulatory loop. (a) Schematic representation of the mock circulatory loop with images of the components; (b) test section with Dacron graft installed and equipped with Carolina Medical magnetic flowmeters and Millar catheter pressure sensors.

and was fixed to rigid cylindrical supports by hose clamps, leaving a free length of 117 mm between the supports (with pre-stretch 1.3). To prevent liquid leakage, a very thin latex film (0.046 mm thick) of negligible stiffness compared to Dacron was placed inside the graft. In order to simulate both upstream and downstream arterial compliance, two compliant chambers (manufactured by BDC Laboratories) were positioned before and after the location of the prosthesis. Each compliance chamber features an approximate total volume of 2.25 L. The loop is filled with salted water (salt 0.9% in volume), while an air pocket is trapped on top of a compliance chamber; this pocket provides compliance as air is compressible and constitutes a pneumatic spring. The stiffness of the spring is proportional to the volume of air, which is adjusted by pneumatic components. A gauge measures the pressure of the air pocket. After the Dacron prosthesis, a pinch valve was installed to introduce arterial resistance to flow. The tuning of the volume of air in the expansion chambers and of the level of squeezing introduced by the pinch valve allows to obtain the desired 100 mmHg mean pressure, the diastolic pressure of about 80 mmHg and the systolic pressure of around 120 mmHg. The tuning must be repeated at every simulated heart rate.

The function of the tank, open to the atmospheric pressure, is to separate the test section from the drawing action of the inlet of the pump, i.e. it separates the arterial tree from the venous system. In fact, the flow in the descending thoracic aorta is determined only by the systolic pumping of the heart and by the Windkessel effect, while the atria of the heart do not provide any suction. In the tank, a heater was installed to maintain the fluid at body temperature.

2.4. Dynamic displacement measurement

Hemodynamic investigations in general assume axisymmetric radial deformation of arterial ducts. In the specific problem, bend-

ing displacements are very relevant, due to the initial deviation of the graft from the perfectly straight configuration and its extremely low axial stiffness. The graft bends by increasing the transmural pressure. Thus, the mean and oscillatory components of pressure induce a lateral bending motion without diameter changes, see Fig. 4(d), superimposed to an axisymmetric motion, see Fig. 4(b), with diameter change (*breathing* motion). The direction along which the bending motion happens cannot be predicted and is given by the initial bending of the graft once installed onto the rigid frame.

Four perpendicular OFV 505/PSV 500 Polytec laser Doppler vibrometers equipped with displacement decoders (sensitivity setting 200 $\mu\text{m}/\text{volt}$) were used simultaneously. Each one pointed at half-length of the prosthesis and measured the displacement in the direction of the laser beam, capturing both bending and axisymmetric dynamic deformation, as shown in Fig. 4(a–e). During an axisymmetric deformation, the sections of the prosthesis are expected to remain circular while all radii change of a same quantity. Therefore, for a purely axisymmetric motion, all lasers would measure identical signals in phase and amplitude. With similar geometric considerations, it can be shown that, for a purely bending motion, one couple of coaxial laser sensors would measure signals identical in amplitude but with opposite phase. Therefore, if the four signals from the lasers are named V_{top} (top), V_{bot} (bottom), V_{left} (left), V_{right} (right), the axisymmetric components of motion in the vertical and axial directions are given by

$$(V_{top} + V_{bot})/2, \quad (V_{left} + V_{right})/2, \quad (5a, b)$$

respectively. The two components of the axisymmetric motion should be equal for a perfectly circular and axisymmetric graft. Differences in the previous expression are introduced by

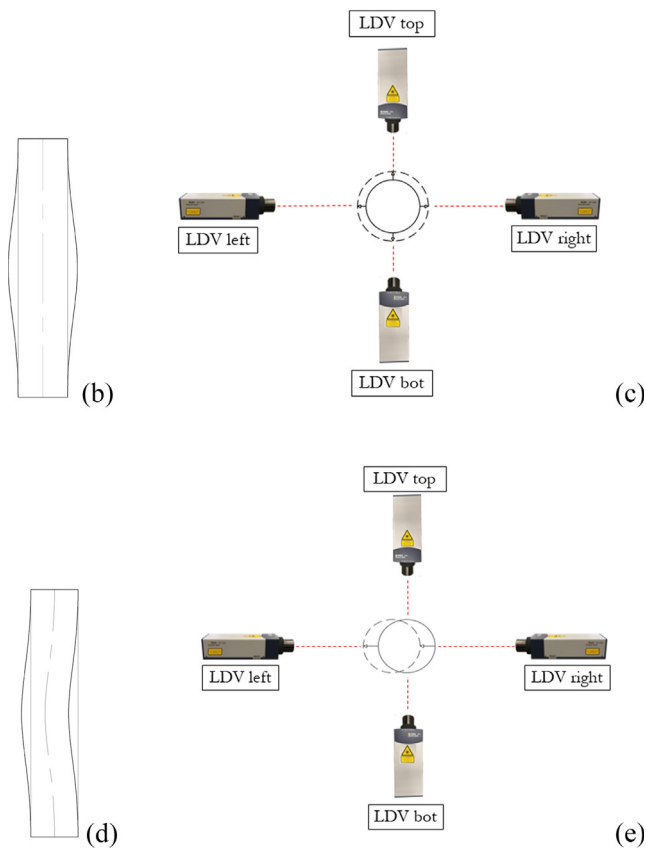
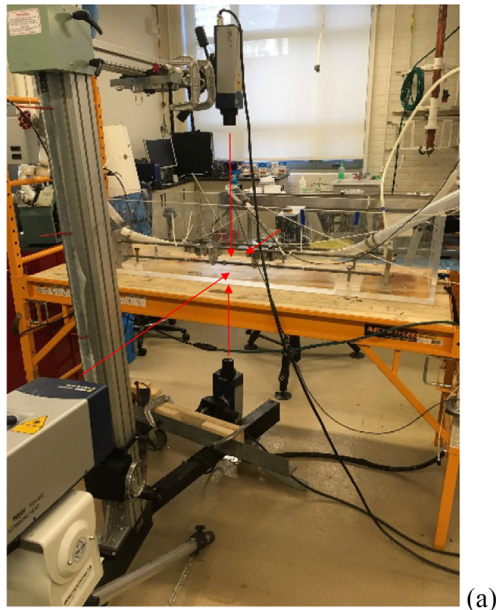


Fig. 4. Measurement of the dynamic deformation of the Dacron graft by using four Polytec laser Doppler vibrometers. (a) Experimental set-up with the four laser Doppler vibrometer heads; (b) axisymmetric (*breathing*) deformation of the graft; (c) measurement of the axisymmetric deformation; (d) bending deformation of the graft; (e) measurement of the bending deformation.

imperfections. The bending components in the two directions are obtained as

$$(V_{top} - V_{bot})/2, \quad (V_{left} - V_{right})/2. \quad (6a, b)$$

A schematic of the laser measurements of axisymmetric and bending motions is shown in Fig. 4(c) and Fig. 4(e), respectively.

3. Results

3.1. Storage modulus and loss factors of woven Dacron

The storage modulus in axial and circumferential direction at different initial pre-stretches is given in Fig. 5(a) and (c), respectively. Fig. 5(a) has been obtained in presence of corrugations, while Fig. 5(c) coincides with the one presented in Amabili et al. (2018). Results indicate that the storage modulus is largely increasing (more than doubling) when passing from static load to 1 Hz of harmonic loading, while a further modest stiffness increase is observed at higher frequencies. A two-order of magnitude difference is observed between storage moduli in the circumferential and axial directions. The corresponding loss factors are given in Fig. 5(b and d).

3.2. Mock circulatory loop

The results obtained for the Dacron graft in the mock circulatory loop are presented for four heart rates: 52, 92, 126 and 164 bpm. These rates correspond roughly to the case of rest, moderate and intense physical activity. A volumetric stroke of 50 cc and a systole-to-diastole ratio of 25/75 were used. The mean, systolic and diastolic pressures were kept similar at different heart rates in order to have the same load acting on the graft at different frequencies.

The measured inlet pressure p_1 , outlet pressure p_2 and pulsating volumetric flow rate are presented in Fig. 6(a) for a heart rate of 52 bpm and are close to standard physiological pressure and flow at rest, including the phase relationship between flow rate and pressure (Mills et al., 1970). The measured systolic pressure is 113 mmHg and the diastolic pressure is 73 mm Hg. This confirms the good performance of the tuned mock circulatory loop. The axisymmetric oscillation is shown in Fig. 6(b). It presents an oscillation amplitude of about 0.07 mm and follows closely the pressures p_1 and p_2 . Fig. 6(c) displays the bending oscillation in the vertical and horizontal directions, which also follow the pressures p_1 and p_2 . The horizontal bending oscillation amplitude is 0.32 mm.

Fig. 7(a–c) presents measures for the graft at 92 bpm. The amplitude of the axisymmetric oscillation is about 0.07 mm and the one of the horizontal bending increases to 0.4 mm; it can be observed that a slightly larger mean pressure was reached in this case (systole 135 mmHg, diastole 93 mmHg) with respect to the case at 52 bpm. It can be concluded that similar breathing and bending oscillations were observed at 52 and 92 bpm.

Results at 126 bpm are presented in Fig. 8(a–c) with horizontal bending oscillations of 0.33 mm (systole 121 mmHg, diastole 86 mmHg) and breathing oscillation of about 0.07 mm.

Finally, the test at 164 bpm is displayed in Fig. 9(a–c) and shows a bending amplitude of 0.37 mm while the axisymmetric vibration is still 0.07 mm; the systolic pressure is 124 mmHg and the diastolic pressure is 86 mmHg, thus close to the 126 and 52 bpm cases.

The typical maximum measurement error for the Millar catheter pressure sensor is 3 mmHg, for the Carolina Medical magnetic flowmeter is 0.3 L/min, for the dynamic displacement is 4 μ m and mostly due to alignment accuracy.

A comparison of the present quasi-static pressurization experiment with those by Bustos et al. (2016b) for a similar, but slightly smaller Dacron graft of 24 mm diameter, is presented in Fig. 10. The relationship between pressure (mmHg) and circumferential stretch λ_θ at midlength of the graft under an axial pre-stretch $\lambda = 1.3$ shows results in reasonable agreement (only two points were measured in the present test). Fig. 10 displays also results for dynamic inflation experiment under pulsatile pressure at 52 bpm (data from Fig. 6b). It is very interesting to see that the

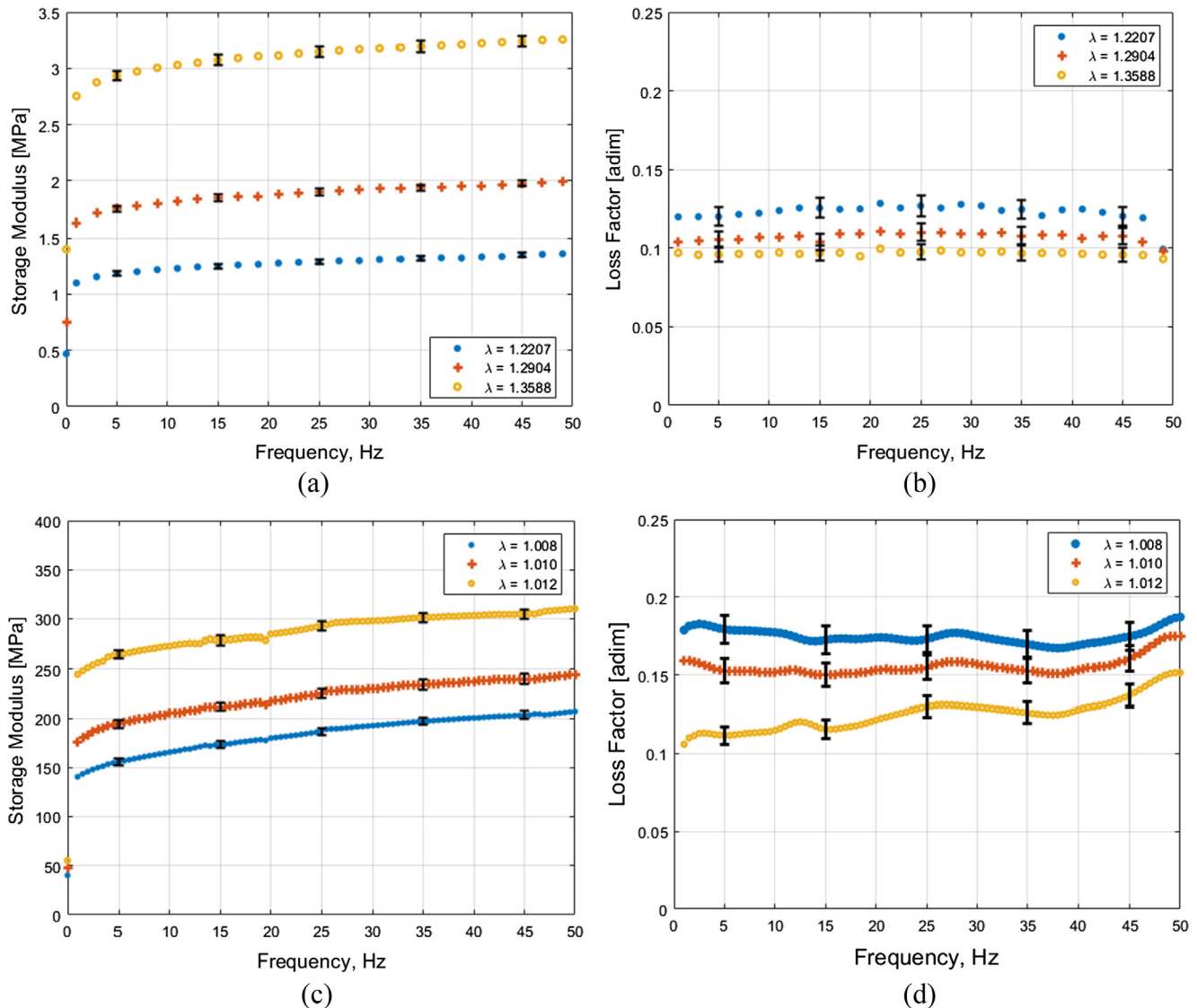


Fig. 5. Storage modulus (from 2nd Piola-Kirchhoff stress and Green's strain) and loss factor versus loading frequency at three different initial pre-stretches λ ; the error bars quantify the estimated measurement errors. (a) Storage modulus of the axial strip; (c) loss factor of the axial strip; (c) storage modulus of the circumferential strip; (d) loss factor of the circumferential strip.

slope of the dynamic pressurization is over three times larger than the quasi-static pressurization. This is directly linked to the ratio between the dynamic stiffness at 0.87 Hz and the static stiffness, both in circumferential direction. Fig. 5(c) shows that the ratio between the dynamic stiffness at 1 Hz and the static stiffness is about 3.5, which is in full agreement with the increase of the slope of the dynamic pressurization curve in Fig. 10.

4. Discussion and conclusions

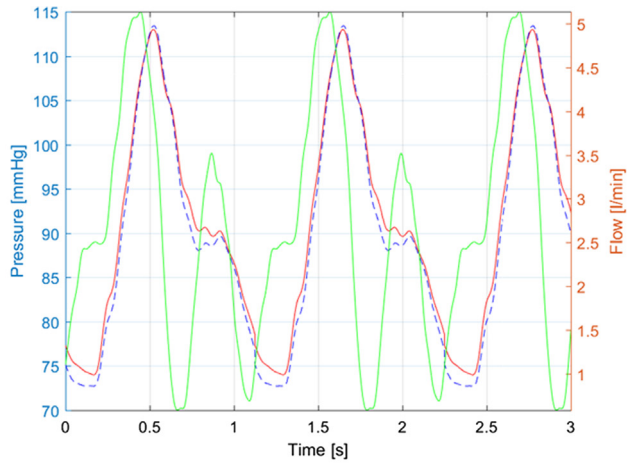
Across the entire set of heart rates, the amplitude of dynamic bending of the Dacron graft observed in the mock circulatory loop was 0.3–0.4 mm. This is about five times larger than the amplitude of the axisymmetric (breathing) oscillation, which has been measured to be around 0.07 mm. The ratio between the axisymmetric oscillation amplitude and the graft radius is 0.5%, which is much smaller than the dynamic change of diameter during *in vivo* blood pulsation in the human descending thoracic aorta, which is reported to be between 8.1 and 2.7%, according to the age (Morrison et al., 2009). Therefore, experimental results indicate a

very strong mismatch between the dynamic expansion of the lumen of the human aorta and that of the Dacron graft, which has an extremely reduced Windkessel effect. This is a potential source of complications for the proper functioning of the heart. In addition, the connection between the human aorta, which expands significantly at any heart beat (especially for younger individuals), and the circumferentially stiff Dacron graft represents a point of significant stress concentration and a potential source of problems. Finally, the bending vibrations observed for the Dacron prosthesis have no counterpart in the human aorta and this is a further point of concern.

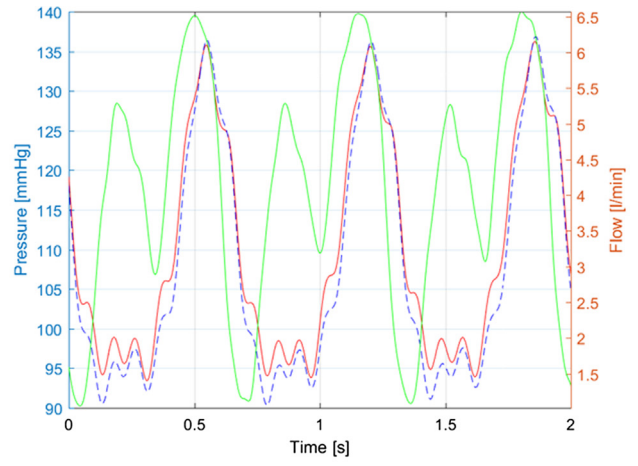
Based on this study, a hypothetical new generation of dynamically compatible aortic grafts should mimic the hyperelastic and viscoelastic material properties of the human aorta and its layered structure in order to reduce the dynamic mismatch observed in the currently used commercial Dacron aortic prostheses.

Conflict of interest statement

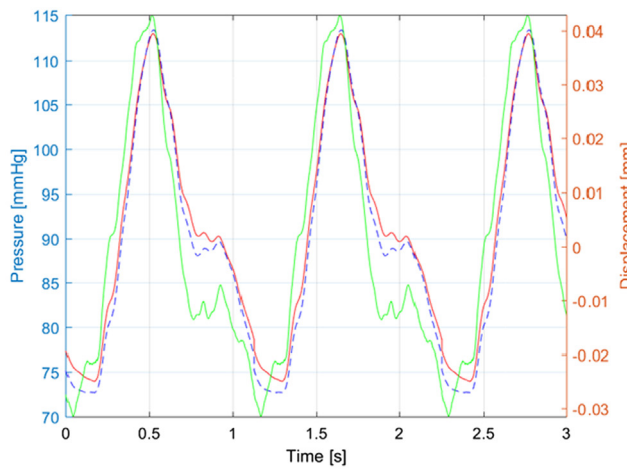
The authors have no conflicts of interest to disclose.



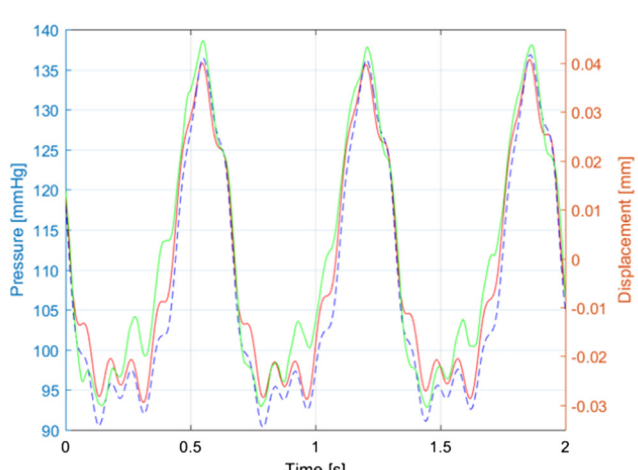
(a)



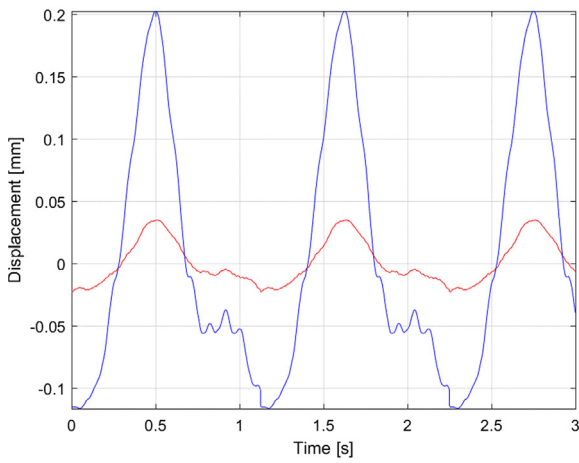
(a)



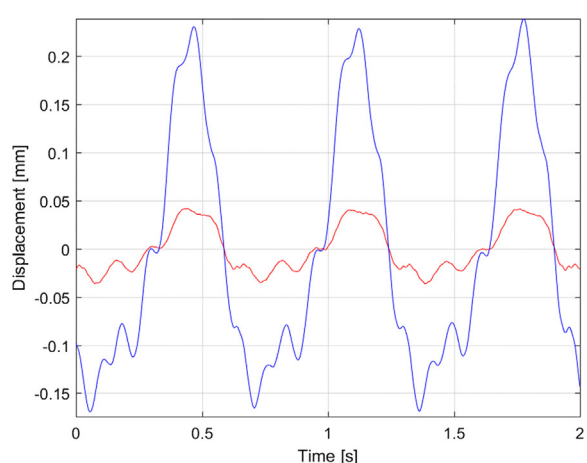
(b)



(b)



(c)



(c)

Fig. 6. Dacron graft at 52 bpm. (a) Inlet pressure (continuous red line), outlet pressure (dashed blue line), volumetric flow rate (continuous green line) versus time; (b) inlet pressure (continuous red line), outlet pressure (dashed blue line), axisymmetric (breathing) dynamic displacement in horizontal direction (green continuous line); (c) bending dynamic displacement: vertical direction (red line), horizontal direction (blue line). (For interpretation of the references to colour in this figure legend, the reader is referred to the web version of this article.)

Fig. 7. Dacron graft at 92 bpm. (a) Inlet pressure (continuous red line), outlet pressure (dashed blue line), volumetric flow rate (continuous green line) versus time; (b) inlet pressure (continuous red line), outlet pressure (dashed blue line), axisymmetric (breathing) dynamic displacement in horizontal direction (green continuous line); (c) bending dynamic displacement: vertical direction (red line), horizontal direction (blue line). (For interpretation of the references to colour in this figure legend, the reader is referred to the web version of this article.)

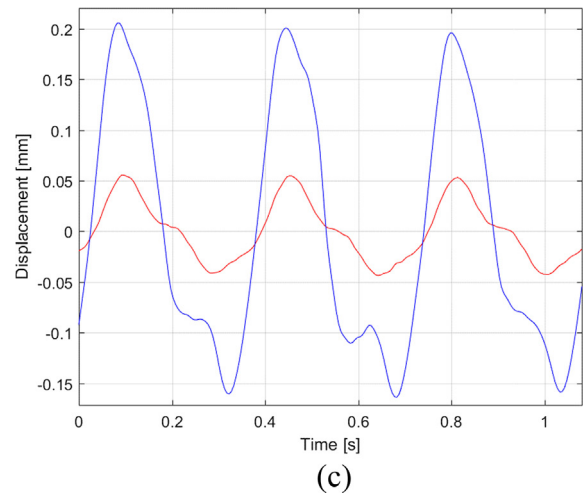
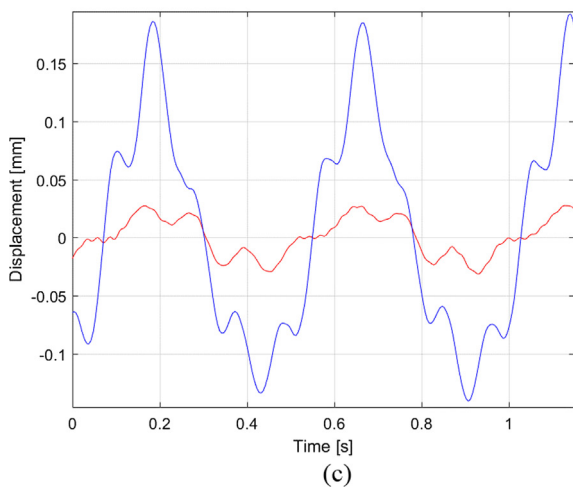
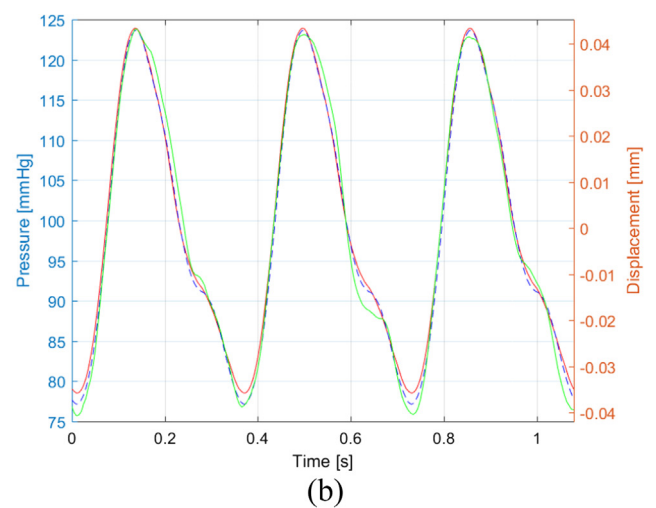
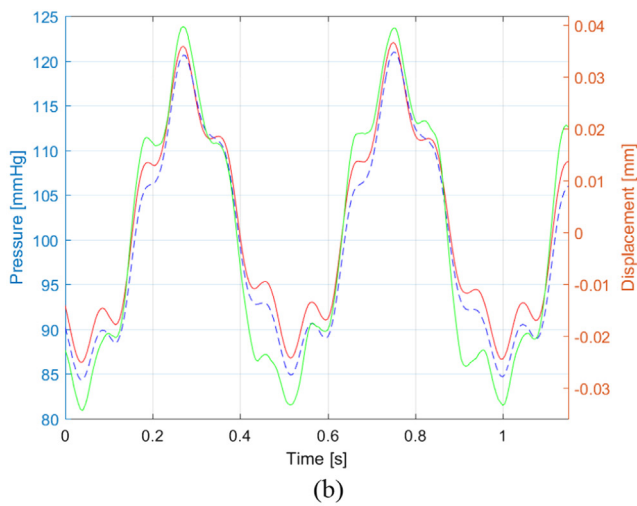
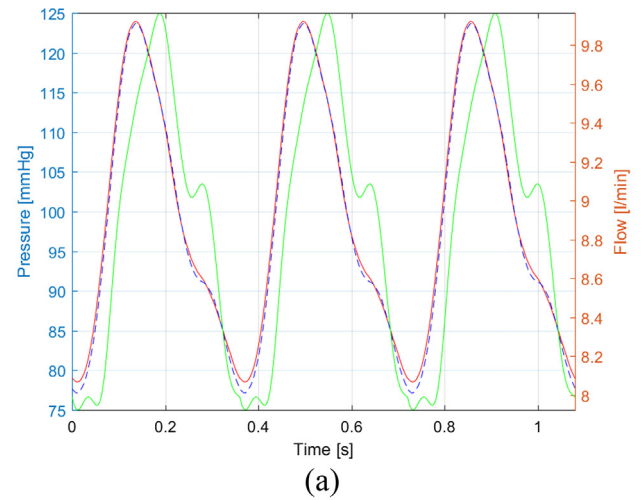
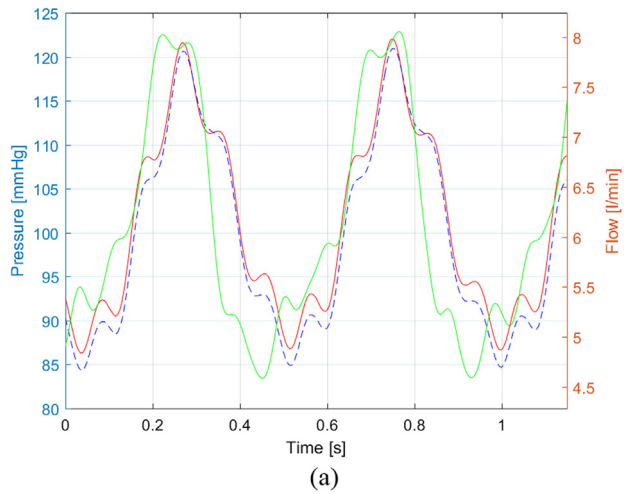


Fig. 8. Dacron graft at 126 bpm. (a) Inlet pressure (continuous red line), outlet pressure (dashed blue line), volumetric flow rate (continuous green line) versus time; (b) inlet pressure (continuous red line), outlet pressure (dashed blue line), axisymmetric (breathing) dynamic displacement in horizontal direction (green continuous line); (c) bending dynamic displacement: vertical direction (red line), horizontal direction (blue line). (For interpretation of the references to colour in this figure legend, the reader is referred to the web version of this article.)

Fig. 9. Dacron graft at 164 bpm. (a) Inlet pressure (continuous red line), outlet pressure (dashed blue line), volumetric flow rate (continuous green line) versus time; (b) inlet pressure (continuous red line), outlet pressure (dashed blue line), axisymmetric (breathing) dynamic displacement in horizontal direction (green continuous line); (c) bending dynamic displacement: vertical direction (red line), horizontal direction (blue line). (For interpretation of the references to colour in this figure legend, the reader is referred to the web version of this article.)

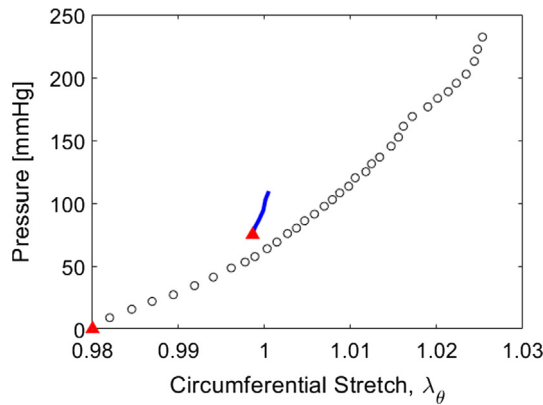


Fig. 10. Relationship between pressure (mmHg) and circumferential stretch λ_θ at midlength for the Dacron graft for axial pre-stretch $\lambda = 1.3$. ○, results for quasi-static inflation experiment by Bustos et al. (2016b) for Dacron graft of 24 mm diameter; ▲, present results for quasi-static inflation experiment for Dacron graft of 28 mm diameter; —, present results for dynamic inflation experiment under pulsatile pressure at 52 bpm for Dacron graft of 28 mm diameter.

Acknowledgments

The authors acknowledge the financial support of the NSERC Discovery Grant, the Canada Foundation for Innovation and the Canada Research Chair programs. We greatly thank Prof. Rosaire Mongrain of McGill University who has kindly provided the original Harvard Apparatus pump used in the experiments.

Appendix A. Measurement errors

The expression for calculating the measurement error for the storage modulus is given by

$$E' = \frac{|\Delta f \pm \Delta f_e|/A}{|\Delta l \pm \Delta l_e|/L} \frac{1}{\lambda^2} \cos(\phi \pm \phi_e), \quad (\text{A1})$$

where Δf_e is the measurement error from the dynamic force sensor, Δl_e is the error from the laser Doppler and ϕ_e is the phase angle error from the data acquisition system. The value of E' is maximized and minimized to get the bounds for the storage modulus. Similarly, for the loss factor the error is expressed as

$$\eta = \tan(\phi \pm \phi_e). \quad (\text{A2})$$

References

- Amabili, M., Balasubramanian, P., Breslavsky, I., Ferrari, G., Tubaldi, E., 2018. Viscoelastic characterization of woven Dacron for aortic grafts by using direction-dependent quasi-linear viscoelasticity. *J. Mech. Behav. Biomed. Mater.* 82, 282–290.
- Bustos, C.A., García-Herrera, C.M., Celentano, D.J., 2016a. Mechanical characterisation of Dacron graft: Experiments and numerical simulation. *J. Biomech.* 49, 13–18.
- Bustos, C.A., García-Herrera, C.M., Celentano, D.J., 2016b. Modelling and simulation of the mechanical response of a Dacron graft in the pressurization test and an end-to-end anastomosis. *J. Mech. Behav. Biomed. Mater.* 61, 36–44.
- Dalsing, M.C., Kevorkian, M., Raper, B., Nixon, C., Lalka, S.G., Cikrit, D.F., Unthank, J.L., Herring, M.B., 1989. An experimental collagen-impregnated Dacron graft: potential for endothelial seeding. *Ann. Vasc. Surg.* 3, 127–133.
- Hasegawa, M., Azuma, T., 1979. Mechanical properties of synthetic arterial grafts. *J. Biomech.* 12, 509–517.
- Horný, L., Netušil, M., Voňavková, T., 2014. Axial prestretch and circumferential distensibility in biomechanics of abdominal aorta. *Biomech. Model. Mechanobiol.* 13, 783–799.
- How, T.V., 1992. Mechanical properties of arteries and arterial grafts. In: Hastings, G.W. (Ed.), *Cardiovascular Biomaterials*. Springer, London, London, pp. 1–35.
- Jayendiran, R., Nour, B., Ruimi, A., 2018. Dacron graft as replacement to dissected aorta: A three-dimensional fluid-structure-interaction analysis. *J. Mech. Behav. Biomed. Mater.* 78, 329–341.
- Lee, J.M., Wilson, G.J., 1986. Anisotropic tensile viscoelastic properties of vascular graft materials tested at low strain rates. *Biomaterials* 7, 423–431.
- Mills, C., Gabe, I., Gault, J., Mason, D., Ross, J., Braunwald, E., Shillingford, J., 1970. Pressure-flow relationships and vascular impedance in man. *Cardiovasc. Res.* 4, 405–417.
- Morrison, T.M., Choi, G., Zarins, C.K., Taylor, C.A., 2009. Circumferential and longitudinal cyclic strain of the human thoracic aorta: age-related changes. *J. Vasc. Surg.* 49, 1029–1036.
- Spadaccio, C., Rainer, A., Barbato, R., Chello, M., Meyns, B., 2013. The fate of large-diameter Dacron® vascular grafts in surgical practice: Are we really satisfied? *Int. J. Cardiol.* 168, 5028–5029.
- Taylor, C.E., Dziczkowski, Z.W., Miller, G.E., 2012. Automation of the harvard apparatus pulsatile blood pump. *J. Med. Devices* 6, 045002-045002-045010.
- Taylor, C.E., Miller, G.E., 2012a. Implementation of an automated peripheral resistance device in a mock circulatory loop with characterization of performance values using simulink simscape and parameter estimation. *J. Med. Devices* 6, 045001-045001-045007.
- Taylor, C.E., Miller, G.E., 2012b. Mock circulatory loop compliance chamber employing a novel real-time control process. *J. Med. Devices* 6, 0450031-0450038.
- Thompson, J.E., 1998. Early history of aortic surgery. *J. Vasc. Surg.* 28, 746–752.
- Tremblay, D., Zigras, T., Cartier, R., Leduc, L., Butany, J., Mongrain, R., Leask, R.L., 2009. A comparison of mechanical properties of materials used in aortic arch reconstruction. *Ann. Thoracic Surg.* 88, 1484–1491.
- Tubaldi, E., Paidoussis, M.P., Amabili, M., 2018. Nonlinear dynamics of dacron aortic prostheses conveying pulsatile flow. *J. Biomech. Eng.* 140, 061004-061004-061012.
- Yeoman, M.S., Reddy, D., Bowles, H.C., Bezuidenhout, D., Zilla, P., Franz, T., 2010. A constitutive model for the warp-weft coupled non-linear behavior of knitted biomedical textiles. *Biomaterials* 31, 8484–8493.